Optimal Multi-Objective Resource Allocation for D2D Underlaying Cellular Networks in Uplink Communications

SIAVASH BAYAT[1], (Member, IEEE), **JALAL JALALI**[2], (Graduate Student Member, IEEE),
ATA KHALILI[1], (Member, IEEE), **MOHAMMAD ROBAT MILI**[2], (Member, IEEE),
SABINE WITTEVRONGEL[2], **AND HEIDI STEENDAM**[2], (Senior Member, IEEE)

[1]Electronics Research Institute, Sharif University of Technology, Tehran 11365-8639, Iran
[2]Department of Telecommunications and Information Processing, TELIN/IMEC, Ghent University, 9000 Ghent, Belgium

Corresponding author: Siavash Bayat (bayat@sharif.edu)

ABSTRACT In this paper, we study a resource allocation problem in orthogonal frequency division multiple access (OFDMA)-based Device-to-Device (D2D) communications. To this end, we propose a multi-objective optimization problem (MOOP) framework, which jointly maximizes the sum rate of D2D users (DUs) and cellular users (CUs) in uplink communications and minimizes the total transmit power. The proposed problem formulation takes into account the minimum data-rates and the maximum transmitted power budget for both DUs and CUs. We transform this MOOP into a single-objective optimization problem (SOOP) using the weighted sum method and then propose an approach to solve this SOOP via a monotonic approach yielding an efficient optimal solution. Furthermore, a suboptimal solution based on the successive convex approximation (SCA) is presented to compromise complexity and performance gain. This is done to reveal that the proposed suboptimal solution closely approaches an optimal solution through simulation analysis. Numerical results unveil an interesting tradeoff between D2Ds CUs and demonstrate the superiority of our proposed solution compared to other baseline schemes.

INDEX TERMS Device-to-Device (D2D), resource allocation, multi-objective optimization problem (MOOP), weighted sum method, monotonic optimization, successive convex approximation (SCA).

I. INTRODUCTION

Device-to-Device (D2D) communication is developed as a new paradigm to enhance network performance and to improve resource utilization in fifth generation (5G) cellular networks and advanced standards. With D2D communications, a direct link can be set up between a pair of D2D users within the cellular coverage without the help of the base station. In the underlay mode (shared spectrum) of D2D communications, the interference mitigation between the D2D users (DUs) and cellular users (CUs) due to the shared spectrum is considered as one of the most critical issues [1].

Most previous works on resource allocation in D2D communications considered a single-objective optimization problem (SOOP) optimizing only D2D or cellular

The associate editor coordinating the review of this manuscript and approving it for publication was Nan Wu.

links [2]–[9]. In [2], the authors maximized the sum data-rate of the D2D pairs when the basic data-rate requirements of all CUs in uplink communication are guaranteed, by optimizing power and subchannel allocation iteratively. In [3], spectral efficiency (SE) and energy efficiency (EE) were separately maximized by a SOOP to strike a balance between energy and spectral efficiency in underlaying D2D communications. In [4], a SOOP was formulated to maximize the total EE in D2D communications underlaying uplink cellular networks when the quality of service of each D2D pair and the transmit power threshold are guaranteed. The problem of relay selection, bandwidth and power allocation was investigated in [5] to enhance the weighted sum EE, while guaranteeing the minimum data-rate requirement for CUs, by exploiting the theory of fractional programming. In [6], the authors studied the energy-efficient resource allocation problem for D2D communication to maximize the minimum weighted EE by decoupling the problem into two sub-problems, i.e., the

subchannel and power allocation. To improve SE and reduce latency, a D2D enabled cloud radio access network was developed in [7], where a distributed approach for mode selection and resource allocation was presented. The problem of joint mode selection and resource allocation to maximize the system sum rate for D2D underlaid cellular communications was studied in [8] and algorithms for centralized and decentralized approaches were considered. The energy-efficient resource allocation problem in the downlink for a D2D communication heterogeneous network incorporating energy harvesting with time slot allocation was investigated in [9]. The authors in [10] considered multi-hop cooperative communications to improve the coverage range of D2D communications underlaying cellular networks while taking into account the network coding (NC). However, the single-objective optimization frameworks in [2]–[10] are not appropriate to consider the tradeoff between DUs and CUs.

In [11], the spectrum allocation problem of D2D enabled cellular networks was investigated, where the cooperative game theory is employed. In [12], the cooperative relaying-based spectrum trading process between the cellular system and D2D link was considered by a principal-agent framework. For such a framework, the authors offered a contract-based cooperative spectrum sharing mechanism to exploit transmission opportunities for the D2D links and obtain the maximum profit of the cellular links. A spectrum sharing mode for D2D communications in cellular networks was presented in [13], where two or more D2D links with exclusive use of sub-bands were allowed to share their sub-bands without consulting the operators. Under this model, the authors designed a game-theoretic model called Bayesian non-transferable utility overlapping coalition formation game to analyze the spectrum sharing problem. In [14], to derive analytical rate expressions, a hybrid network model of D2D enhanced cellular networks was studied, where a random spatial Poisson point process modeled the positions of mobiles. The authors in [14] considered two D2D association approaches, namely the simultaneous and sequential D2D associations, where both schemes aimed to concurrently maximize the desired link quality and minimize the effect of interference effect at D2D receivers.

The MOOP framework studies the correlation between conflicting objectives in wireless systems [15]–[17]. In this regard, a MOOP tradeoff was studied in [15] to compromise between EE and SE. This problem was transformed into a SOOP via the epsilon method, and a two-stage iterative solution was proposed. Furthermore, in [16], a multi-objective cell association optimization for arranging several D2D links in a multi-cell network based on the fractional frequency reuse scheme was considered. However, because of the interference experienced by DUs in each cell, and also the effect of the received interfering power from CUs on the DUs' achievable rate, a non-trivial tradeoff between DUs and CUs would be expected. Derivation of a tradeoff between DUs and CUs can lead to an interesting optimization problem that has not been addressed in the literature yet.

Contrary to [2]–[9], [15], [16], we investigate in this paper the performance tradeoff between DUs and CUs in OFDMA D2D networks underlaying CUs, by optimizing the EE and throughput using a MOOP. This performance tradeoff can enhance the load balancing between DUs and CUs. For balancing the load between different DUs and CUs, a service provider utilizes adjustable weighting parameters in executing the resource allocation policy to guarantee a better degree of freedom while providing a fairness among the DUs and CUs. To this end, we formulate in this paper a MOOP framework that jointly maximizes the uplink sum rates of CUs and DUs and minimizes the total transmit power at DUs and CUs. To the best of our knowledge, this has not been investigated in literature before. The contributions of this paper are summarized as follows:

- We formulate a MOOP to simultaneously maximize the sum data-rate and minimize the transmit power for both CUs and DUs while constraining on the minimum data-rate requirement and feasibility of the transmitted powers.
- To do so, we first apply the weighted sum method, which transforms the problem into a SOOP. Then, we propose an optimal approach that assigns subchannels to both CUs and DUs, and also allocates power to them. Besides, a sub-optimal solution based on successive convex approximation (SCA) is proposed to strike a balance between complexity and performance gain which demonstrates much lower compared to monotonic approach. Based on the weights given to the CUs and DUs, we can determine the priority being assigned to DUs and CUs, respectively.
- In the numerical results, we show the superiority of the MOOP formulation compared with SOOP in a special region, where the data-rate of only DUs is maximized, i.e., no tradeoff exists between DUs and CUs. Using this tradeoff, we are able to exploit the whole capability of network resources while considering the feasibility of the transmit power for both DUs and CUs together with the minimum required data-rate of both DUs and CUs.

The remainder of the paper is organized as follows. Section II introduces the system model and Section III formulates and analyzes the MOOP. An optimal and suboptimal solution are discussed in Section IV. The complexity analysis of the solutions are covered in Section V. Numerical results are given in Section VI. Finally, we conclude the paper in Section VII.

II. SYSTEM MODEL

We consider an uplink (UL) single macro cell OFDMA-based cellular network as shown in Fig. 1. This cell has one base station to serve M CUs, where K D2D links (DUs), i.e., pairs of D2D users, exist in this cell. The set of CUs and DUs are denoted as $\mathcal{M} = \{1, 2, , \ldots, M\}$ and $\mathcal{K} = \{1, 2, \ldots, K\}$,
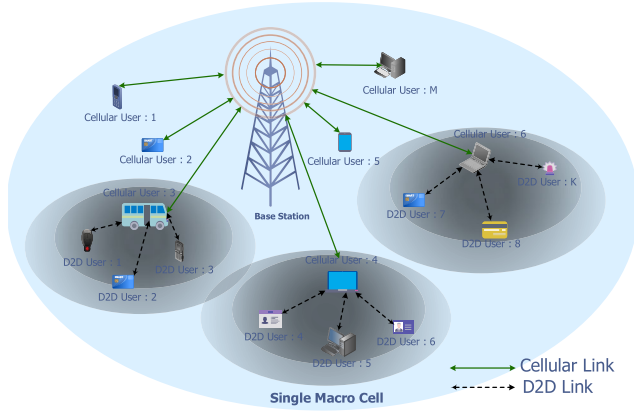
FIGURE 1. The system model of an uplink single macro cell OFDMA-based cellular network with one base station to serve *M* CUs and *K* DUs. In this figure, the green arrow shows the cellular transmission link between the base station and the CUs, while the dotted line indicates the D2D links.

respectively. The bandwidth of B Hz is divided into N orthogonal subchannels so that each subchannel has a bandwidth of $B_c = B/N$ Hz, where the subchannel set is denoted as $\mathcal{N} = \{1, 2, \ldots, N\}$. The subchannels are modeled as block flat-fading channels, hence they remain constant during each time slot, but may vary independently from one time slot to another. Nevertheless, all the subcarriers are considered to be entirely orthogonal to one another, and no inter-subcarrier interference exists. Furthermore, we assume that perfect channel state information (CSI) is available at the resource allocator for both CUs and DU to devise the resource allocation policy so as to unveil the performance analysis of the considered network.[1] Hence, the obtained rates using our proposed algorithms can be considered as upper bounds on the achievable rates for the case where the channel needs to be estimated. For ease of readability, we first present some of the essential parameters that are used to define the system model:

- $h_{k,\mathrm{BS}}^n(t)$: The instantaneous channel power gain between the k-th DU and the base station in subchannel n and time slot t.
- $\hat{h}_{k',k}^{'n}(t)$: The instantaneous channel power gain from the k'-th DU transmitter to the k-th DU receiver on subchannel n and time slot t.
- $g_{m,\mathrm{BS}}^n(t)$: The instantaneous channel power gain between the m-th CU and the base station in subchannel n and time slot t.
- $g_{m,k}^{'n}(t)$: The instantaneous channel power gain between the m-th CU and the k-th DU receiver on subchannel n and time slot t.[2]

---

[1] It is assumed the base station transmits orthogonal preambles, pilot signals, to the users in the DL direction. Each user then estimates the CSI and transfers this information back to the base station through a feedback channel. Subsequently, the corresponding base station monitors the sounding reference signals communicated by users and grants the CSI to the centralized controller for the resource allocation design.

[2] Hereafter, the time index t is removed to simplify the notations.

- p_k^n: The transmitted power from the k-th DU in the subchannel n.
- $\hat{p}_m^n$: The corresponding transmitted power for the m-th CU in the subchannel n.
- ψ_m^n: The binary variable indicator for subchannel allocation in the cellular network with $\psi_m^n = 1$ if subchannel n is allocated to CU m and $\psi_m^n = 0$, otherwise. That is,

$$\psi_m^n = \begin{cases} 1, & \text{if subchannel } n \text{ is allocated to CU } m, \\ 0, & \text{otherwise.} \end{cases}$$

- φ_k^n: The binary variable for subchannel allocation in the D2D network with $\varphi_k^n = 1$ if subchannel n is allocated to DU k and $\varphi_k^n = 0$, otherwise. That is,

$$\varphi_k^n = \begin{cases} 1, & \text{if subchannel } n \text{ is allocated to DU } k, \\ 0, & \text{otherwise.} \end{cases}$$

Then, the instantaneous received signal-to-interference-plus-noise ratio (SINR) at the k-th DU receiver on subchannel n can be written as:

$$\mathrm{SINR}_{k,\mathrm{DU}}^n = \frac{\varphi_k^n p_k^n h_k^n}{N_0 B_c + \sum\limits_{m=1}^{M} \psi_m^n \hat{p}_m^n g_m^{'n} + \sum\limits_{\substack{k'=1, \\ k' \neq k}}^{K} \varphi_{k'}^n p_{k'}^n \hat{h}_{k',k}^{'n}}, \quad (1)$$

where $g_m^{'n}$ is the instantaneous channel power gain between the m-th CU and the k-th DU receiver on subchannel n and $\sum\limits_{m=1}^{M} \psi_m^n \hat{p}_m^n g_m^{'n}$ is the interference term arising from cellular links. Furthermore, $\sum\limits_{k'=1, k' \neq k}^{K} \varphi_{k'}^n p_{k'}^n \hat{h}_{k',k}^{'n}$ denotes the interference from other D2D pairs, in which $\hat{h}_{k',k}^{'n}$ is the instantaneous channel power gain from the k'-th DU transmitter to the k-th DU receiver on subchannel n. It should be noted that in formula (1), N_0 is the flat noise power spectral density (of an additive white Gaussian noise (AWGN) random process with zero mean and variance σ^2) in all frequencies.

In addition, the instantaneous received SINR at the m-th CU in subchannel n is given by:

$$\mathrm{SINR}_{m,\mathrm{CU}}^n = \frac{\psi_m^n \hat{p}_m^n g_m^n}{N_0 B_c + \sum\limits_{k=1}^{K} \varphi_k^n p_k^n \hat{h}_k^{'n}}, \quad (2)$$

where $\hat{h}_k^{'n}$ is the instantaneous power gain of the channel between the k-th DU transmitter and the CU m on subchannel n. In (2), the term $\sum\limits_{k=1}^{K} \varphi_k^n p_k^n \hat{h}_k^{'n}$ corresponds to the interference term from D2D links.

Let us now define $\boldsymbol{\varphi} \in \mathbb{Z}^{KN \times 1}$ and $\boldsymbol{\psi} \in \mathbb{Z}^{MN \times 1}$ as the vectors of subchannel assignment variables in D2D and cellular networks, respectively. Further, the vectors containing total transmit power in D2D and cellular networks are $\mathbf{p} \in \mathbb{R}^{KN \times 1}$ and $\hat{\mathbf{p}} \in \mathbb{R}^{MN \times 1}$, which show the collections of power allocation variables in these networks. According to

the famous Shannon capacity formula, the data-rate of the k-th DU over the subcarrier n can be written as:

$$R_{\text{DU},k}(\boldsymbol{\varphi}, \mathbf{p}) = \sum_{n=1}^{N} \log_2(1 + \text{SINR}_{k,\text{DU}}^n). \tag{3}$$

Similarly, we can define the data-rate of the m-th CU over the subcarrier n as:

$$R_{\text{CU},m}(\boldsymbol{\psi}, \hat{\mathbf{p}}) = \sum_{n=1}^{N} \log_2(1 + \text{SINR}_{m,\text{CU}}^n). \tag{4}$$

III. MOOP FORMULATION

In this section, to find a tradeoff between DUs and CUs on the system performance, we formulate a MOOP in which jointly the sum rate of the DUs, R_{DU}, and that of the CUs, R_{CU}, are maximized and the total transmit powers of DUs and CUs, P_{DU} respectively P_{CU}, are minimized. The aim of the proposed MOOP framework is to obtain an efficient power allocation as well as subchannel assignment strategy to balance between an as large as possible data-rate and an as small as possible transmit power of DUs and CUs in a fading environment. This joint optimization can be formulated through the following MOOP:

$$\max_{\{\mathbf{p}, \hat{\mathbf{p}}, \boldsymbol{\varphi}, \boldsymbol{\psi}\}} \quad R_{\text{DU}} = \sum_{k=1}^{K} R_{\text{DU},k}(\boldsymbol{\varphi}, \mathbf{p}) \tag{5a}$$

$$\max_{\{\mathbf{p}, \hat{\mathbf{p}}, \boldsymbol{\varphi}, \boldsymbol{\psi}\}} \quad R_{\text{CU}} = \sum_{m=1}^{M} R_{\text{CU},m}(\boldsymbol{\psi}, \hat{\mathbf{p}}) \tag{5b}$$

$$\min_{\{\mathbf{p}, \hat{\mathbf{p}}, \boldsymbol{\varphi}, \boldsymbol{\psi}\}} \quad P_{\text{DU}} = \sum_{k=1}^{K} \sum_{n=1}^{N} \varphi_k^n p_k^n \tag{5c}$$

$$\min_{\{\mathbf{p}, \hat{\mathbf{p}}, \boldsymbol{\varphi}, \boldsymbol{\psi}\}} \quad P_{\text{CU}} = \sum_{m=1}^{M} \sum_{n=1}^{N} \psi_m^n \hat{p}_m^n \tag{5d}$$

$$\text{s.t. } C_1 : \sum_{n=1}^{N} \varphi_k^n p_k^n \leq P_{\text{max},\text{DU}}, \tag{5e}$$

$$C_2 : \sum_{n=1}^{N} \psi_m^n \hat{p}_m^n \leq P_{\text{max},\text{CU}}, \tag{5f}$$

$$C_3 : R_{\text{DU},k} \geq R_{\text{min},k,\text{DU}}, \quad \forall k \in \mathcal{K}, \tag{5g}$$

$$C_4 : R_{\text{CU},m} \geq R_{\text{min},m,\text{CU}}, \quad \forall m \in \mathcal{M}, \tag{5h}$$

$$C_5 : \sum_{m=1}^{M} \psi_m^n \leq 1, \quad \forall n \in \mathcal{N}, \tag{5i}$$

$$C_6 : \varphi_k^n \in \{0, 1\}, \quad \forall k \in \mathcal{K}, n \in \mathcal{N}, \tag{5j}$$

$$C_7 : \psi_m^n \in \{0, 1\}, \quad \forall m \in \mathcal{M}, n \in \mathcal{N}. \tag{5k}$$

In the optimization problem (5), C_1 (5e) and C_2 (5f) show that the total transmit power of should not exceed their maximum threshold, which are denoted by $P_{\text{max},\text{DU}}$ and $P_{\text{max},\text{CU}}$. The minimum data-rate requirement for each DU and CU, $R_{\text{min},\text{DU}}$ and $R_{\text{min},\text{CU}}$, are assured in constraints C_3 (5g) and C_4 (5h), respectively. Constraint C_5 (5i) sanctions each subcarrier to be allocated to at most one CU. Finally, C_6 (5j)

and C_7 (5k) constraints affirm that the subcarrier indicator variable necessitates only binary values.

Note that optimization problem (5) is a mixed-integer nonlinear programming (MINLP) because of the presence of the binary constraints, multiplication of two variables, and the inter-cell interference present in the data-rate functions in both CUs and DUs [21]–[24].

In the following section, we first restate the problem (5) as a mathematically tractable form to optimize the challenging objective functions. We also guarantee a minimum data-rate for both CUs and DUs, and ensure a maximum power budget for all users is fulfilled. We propose optimal and suboptimal resource allocation algorithms, which have a polynomial-time computational complexity to compromise between complexity and system performance.

IV. PROPOSED SOLUTION

A technique to solve a MOOP is the weighted sum method [20] that linearly combines the competing objective functions into a single objective function. This can formally be stated as follows:

$$\max_{\{\mathbf{p}, \hat{\mathbf{p}}, \boldsymbol{\varphi}, \boldsymbol{\psi}\}} \quad \frac{\alpha}{\omega_\alpha} R_{\text{CU}} + \frac{\beta}{\omega_\beta} R_{\text{DU}} - \frac{\gamma}{\omega_\gamma} P_{\text{DU}} - \frac{\delta}{\omega_\delta} P_{\text{CU}} \tag{6a}$$

$$\text{s.t. } C_1(5e) - C_8(5k), \tag{6b}$$

where α, β, γ, and δ denote the weighting coefficients indicating the importance of the different objectives.[3] In the following, to solve the highly nonconvex optimization problem (6) globally, we apply an approach which deals with subchannel assignment and power allocation as follows.

A. OPTIMAL SOLUTION

To obtain the global optimal solution of (6), we use a global optimization approach known as the monotonic optimization method. By using monotonicity or hidden monotonicity in the objective function as well as constraints, this method guarantees the convergence. Some necessary definitions and results related to monotonic are given as [27]–[32]:

Definition 1 (Box): A box with vertex $\mathbf{z}$ is defined as the hyper rectangle $[\mathbf{0}, \mathbf{z}] = \{\mathbf{x} \mid \mathbf{0} \leq \mathbf{x} \leq \mathbf{z}\}$ for given any vector $\mathbf{z}$.

Definition 2 (Normal Set): An infinite set $Z \subset \mathbb{R}_+^{N+1}$ in a normal set when for any given element $\mathbf{z} \in Z$, the box $[\mathbf{0}, \mathbf{z}] \subset Z$.

Definition 3 (Monotonic Optimization): A polyblock with vertex set υ is defined as the union of all boxes $[\mathbf{0}, \mathbf{z}]$, $\mathbf{z} \in \upsilon$ for given any finite set $\upsilon \subset \mathbb{R}_+^{N+1}$.

Definition 4 (Monotonicity in $\mathbb{R}^N$): For $\mathbf{y}_1 \succeq \mathbf{y}_2$, if $f(\mathbf{y}_1) \succeq f(\mathbf{y}_2)$, then, any function $f : \mathbb{R}^N \rightarrow \mathbb{R}$ is monotonically increasing ($\succeq$ is component-wise ordering).

Definition 5 (Projection): The projection of $\mathbf{z}$ onto the boundary of Z, i.e., $\Phi(\mathbf{z}) = \alpha\mathbf{z}$ in which

---

[3]Note that ω_α, ω_β, ω_γ, and ω_δ are the normalization factors to make the four terms in the expression dimensionless, where the addition of the rate and the power becomes meaningful. It should be noted that for the weighting coefficients we have $\frac{\alpha}{\omega_\alpha} + \frac{\beta}{\omega_\beta} + \frac{\gamma}{\omega_\gamma} + \frac{\delta}{\omega_\delta} = 1$.
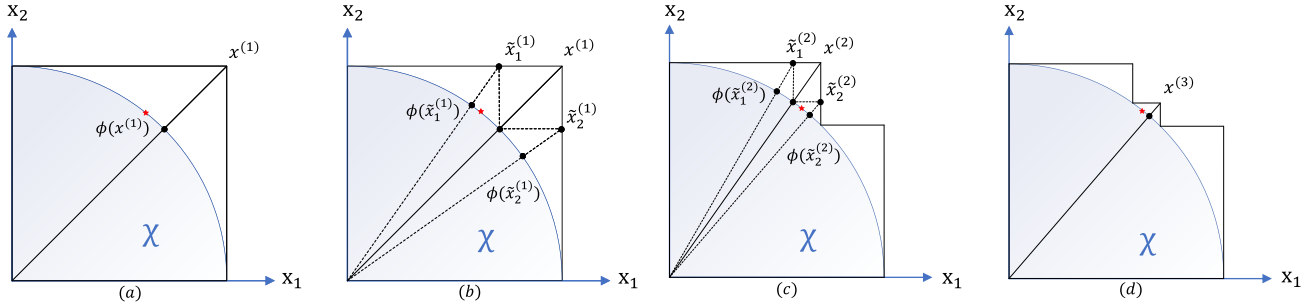
FIGURE 2. Visualization of the outer Polyblock approximation algorithm. As seen, the outer Polyblock approximation algorithm constructs a nested sequence of polyblocks which approximates $\mathcal{X}$ from above. The objective function is maximized by approximating the performance region $\mathcal{X}$ (around the optimal point) from above employing a polyblock. The approximation is enhanced iteratively, and parts that cannot restrain the optimal point are not used.

$\alpha = \max \{\beta \mid \beta \mathbf{z} \in Z\}$ and $\beta \in \mathbb{R}_+$ for given any non-empty normal set $Z \subset \mathbb{R}_+^{N+1}$ and any vector $\mathbf{z} \in \mathbb{R}_+^{N+1}$.

To facilitate the presentation, we define the following relations:

$$0 \leq u_{m,k}^n \leq 1 + \frac{\tilde{p}_m^n g_m^n}{N_0 B_c + \sum_{k=1}^k \bar{q}_k^n \hat{h}_k'^n}, \tag{7}$$

$$0 \leq v_{k,m}^n \leq 1 + \frac{\bar{q}_k^n h_k^n}{N_0 B_c + \sum_{m=1}^M \tilde{p}_m^n g_m'^n + \sum_{k' \neq k} \bar{q}_{k'}^n \hat{h}_{k',k}'^n} \tag{8}$$

where $\tilde{p}_m^n = \psi_m^n \hat{p}_m^n$ and $\bar{q}_k^n = \varphi_k^n p_k^n$. The right-hand side of both relations (7) and (8) are the terms inside the logarithmic functions in (1) and (2), respectively. Now, we redefine the objective function of the optimization problem in (6) as follows:

$$\mathcal{W}(\mathbf{p}, \hat{\mathbf{p}}, \boldsymbol{\varphi}, \boldsymbol{\psi}) = \sum_{n=1}^N \sum_{m=1}^M \sum_{k=1}^K \left(\log_2(u_{m,k}^n)^{\frac{\alpha}{\omega_\alpha}} + \log_2(v_{m,k}^n)^{\frac{\beta}{\omega_\beta}} - \frac{\gamma}{\omega_\gamma} \frac{\tilde{p}_m^n}{M} - \frac{\delta}{\omega_\delta} \frac{\bar{q}_k^n}{K} \right), \tag{9}$$

then, the optimization problem (6) can be restated as:

$$\max_{\{\mathbf{p}, \hat{\mathbf{p}}, \boldsymbol{\varphi}, \boldsymbol{\psi}\}} \mathcal{W}(\mathbf{p}, \hat{\mathbf{p}}, \boldsymbol{\varphi}, \boldsymbol{\psi}) \tag{10a}$$

$$\text{s.t. } \dot{C}_1 : \sum_{n=1}^N \bar{q}_k^n \leq P_{\max,\text{DU}}, \tag{10b}$$

$$\dot{C}_2 : \sum_{n=1}^N \tilde{p}_m^n \leq P_{\max,\text{CU}}, \tag{10c}$$

$$\dot{C}_3 : \tilde{p}_m^n \geq 0, \quad \forall m \in \mathcal{M}, n \in \mathcal{N}, \tag{10d}$$

$$\dot{C}_4 : \bar{q}_k^n \geq 0, \quad \forall k \in \mathcal{K}, \in \mathcal{N}, \tag{10e}$$

$$\dot{C}_5 : \sum_{n=1}^N \log_2(u_{m,k}^n) \geq R_{\min,m,\text{CU}}, \quad \forall m \in \mathcal{M}, \tag{10f}$$

$$\dot{C}_6 : \sum_{n=1}^N \log_2(v_{m,k}^n) \geq R_{\min,k,\text{DU}}, \quad \forall k \in \mathcal{K}, \tag{10g}$$

$$C_5(5i) - C_7(5k), \tag{10h}$$

where $\tilde{\mathbf{p}} \in \mathbb{R}^{2MN \times 1}$ and $\bar{\mathbf{q}} \in \mathbb{R}^{2KN \times 1}$ are the collection of all $\tilde{p}_m^n$ and $\bar{q}_k^n$. Subsequently, we define:

$$f_e(\tilde{\mathbf{p}}, \bar{\mathbf{q}}) = \begin{cases} N_0 B_c + \sum_{k=1}^K \bar{q}_k^n \hat{h}_k'^n + \tilde{p}_m^n g_m^n, \ e = \Delta, \\ N_0 B_c + \sum_{m=1}^M \tilde{p}_m^n g_m'^n + \sum_{\substack{k'=1, \\ k' \neq k}}^K \bar{q}_{k'}^n \hat{h}_{k',k}'^n \\ \quad + \bar{q}_k^n h_k^n, \ e = \frac{\mathcal{E}}{4} + \Delta, \\ \exp(\frac{\tilde{p}_k^n}{M}), \ e = \frac{\mathcal{E}}{2} + \Delta, \\ \exp(\frac{\bar{q}_m^n}{K}), \ e = \frac{3\mathcal{E}}{4} + \Delta, \end{cases} \tag{11}$$

$$g_e(\tilde{\mathbf{p}}, \bar{\mathbf{q}}) = \begin{cases} N_0 B_c + \sum_{k=1}^K \bar{q}_k^n \hat{h}_k'^n, \ e = \Delta, \\ N_0 B_c + \sum_{m=1}^M \tilde{p}_m^n g_m'^n + \sum_{\substack{k'=1, \\ k' \neq k}}^K \bar{q}_{k'}^n \hat{h}_{k',k}'^n, \\ \quad e = \frac{\mathcal{E}}{4} + \Delta, \\ 1, e = \frac{\mathcal{E}}{2} + \Delta, \\ 1, e = \frac{3\mathcal{E}}{4} + \Delta, \end{cases} \tag{12}$$

where $\Delta = (n-1)MK + (m-1)K + k$ and $\mathcal{E} = 4KMN$. Let us define $\mathbf{x} = [x_1, \ldots, x_{\mathcal{E}}]^T = [u_{1,1}^1, \ldots, u_{M,K}^N, v_{1,1}^1, \ldots, v_{M,K}^N, \exp(\frac{\tilde{p}_1^1}{M}), \ldots, \exp(\frac{\tilde{p}_K^N}{M}), \exp(\frac{\bar{q}_1^1}{K}), \ldots, \exp(\frac{\bar{q}_M^N}{K})]^T$. Then, the original monotonic form of the primary optimization problem (10a) can be written as:

$$\max_{\mathbf{x} \in \mathcal{Z}} \sum_{j=1}^{\mathcal{E}} \log_2(x_j)^{\mu_j}, \tag{13}$$

where the μ_j's are the corresponding weights for each sum rate and total transmit powers, i.e, $\mu_j = \frac{\alpha}{\omega_\alpha}, \forall j \in \{1, \ldots, \frac{\mathcal{E}}{4}\}$, $\mu_j = \frac{\beta}{\omega_\beta}, \forall j \in \{\frac{\mathcal{E}}{4} + 1, \ldots, \frac{\mathcal{E}}{2}\}$, $\mu_j = -\frac{\gamma}{\omega_\gamma}, \forall j \in \{\frac{\mathcal{E}}{2} + 1, \ldots, \frac{3\mathcal{E}}{4}\}$, $\mu_j = -\frac{\delta}{\omega_\delta}$, and $\forall j \in \{\frac{3\mathcal{E}}{4} + 1, \ldots, \mathcal{E}\}$. Moreover, the feasible set $\mathcal{X}$ in (13) can be expressed as:

$$\mathcal{X} = \{\mathbf{x} \mid 1 \leq x_j \leq \frac{f_j(\tilde{\mathbf{p}}, \bar{\mathbf{q}})}{g_j(\tilde{\mathbf{p}}, \bar{\mathbf{q}})}, (\tilde{\mathbf{p}}, \bar{\mathbf{q}}) \in \mathcal{P}, (\boldsymbol{\varphi}, \boldsymbol{\psi}) \in \mathcal{S}\}, \tag{14}$$

where the feasible sets $\mathcal{P}$ and $\mathcal{S}$ are spanned by all the constraints of $\dot{C}_1$(10b)-$\dot{C}_4$(10e), $C_5 - C_8$(10h). Moreover, $\mathcal{G}$ is the feasible set which is spanned by constraints $\dot{C}_5$(10f) and $\dot{C}_6$(10g). Since the objective function and all constraints in the problem (10) are monotonic increasing functions, the outer polyblock approximation method can be applied to obtain a globally optimal solution that would be at the boundary of $\mathcal{Z} = \mathcal{X} \cap \mathcal{G}$ [31]. Hence, we make a sequence of polyblocks to reach the boundary of the feasible set. To do this, first a polyblock $\mathcal{B}^{(1)}$ with a vertex set $\mathcal{H}^{(1)}$ is built that includes just one vertex $\mathbf{x}^{(1)}$ and the feasible set $\mathcal{Z} = \mathcal{X} \cap \mathcal{G}$. Based on $\mathcal{B}^{(1)}$, a new smaller polyblock $\mathcal{B}^{(2)}$ is built by substituting $\mathbf{x}^{(1)}$ with new vertices $\tilde{\mathcal{H}}^{(1)} = \{\tilde{\mathbf{x}}_1^{(1)}, \tilde{\mathbf{x}}_2^{(1)}, \ldots, \tilde{\mathbf{x}}_{\mathcal{E}}^{(1)}\}$ where $\tilde{\mathbf{x}}_j^{(1)}$ can be obtained by the following relation $\tilde{\mathbf{x}}_j^{(1)} = \mathbf{x}^{(1)} - (x_j^{(1)} - \phi_j(\mathbf{x}^{(1)}))\mathbf{v}_j$. Specifically, $\mathbf{v}_j$ is a unit vector that has a nonzero value at j-th index, $\Phi(\mathbf{x}^{(1)}) \in \mathbb{C}^{\mathcal{E} \times 1}$ is the projection of vertex $\mathbf{x}^{(1)}$ at the boundary of feasible set $\mathcal{X}$ whose j-th element is $\phi_j(\mathbf{x}^{(1)})$. Therefore, the new vertex set $\mathcal{H}^{(2)}$ related to the polyblock $\mathcal{B}^{(2)}$ can be obtained by $\mathcal{H}^{(2)} = (\mathcal{H}^{(1)} - \mathbf{x}^{(1)}) \cup \tilde{\mathcal{H}}^{(1)}$. Moreover, the corresponding vertex can be found by the following maximization problem $\mathbf{x}^{(2)} = \underset{\mathbf{x} \in \mathcal{H}^{(2)} \cap \mathcal{G}}{\arg\max} \{\sum_{j=1}^{\mathcal{E}} \log_2(\phi_j(\mathbf{x}))^{\mu_j}\}$. In a similar manner, new smaller polyblocks can be built one after another to approach the feasible set, i.e., $\mathcal{Z} \subset \ldots \subset \mathcal{B}^{(2)} \subset \mathcal{B}^{(1)}$. As the system utility function is increasing in this optimization problem, the optimum of the objective function is achieved using a proper vertex. This is the fundamental concept behind the outer Polyblock approximation algorithm; if a polyblock approximates $\mathcal{X}$, then proper vertices of this polyblock approximate the strong Pareto boundary. The outer Polyblock approximation algorithm does this via constructing a nested sequence of polyblocks, which approximates $\mathcal{X}$ from above. This approximation procedure is visualized in Fig. 2. The outer Polyblock approximation method is presented in **Algorithm 1**. Furthermore, $\Phi(\mathbf{x}^{(k)}) = \gamma \mathbf{x}^{(k)}$ is the projection on the boundary of feasible set which can be attained as follows:

$$\gamma = \max\{\alpha \mid \alpha \mathbf{x} \in \mathcal{X}\}$$
$$= \max\{\alpha \mid \alpha \leq \min_{1 \leq e \leq \mathcal{E}} \frac{f_e(\tilde{\mathbf{p}}, \bar{\mathbf{q}})}{x_e^{(k)} g_e(\tilde{\mathbf{p}}, \bar{\mathbf{q}})}, (\tilde{\mathbf{p}}, \bar{\mathbf{q}}) \in \mathcal{P}\}$$
$$= \max_{(\tilde{\mathbf{p}}, \bar{\mathbf{q}}) \in \mathcal{P}} \min_{1 \leq e \leq \mathcal{E}} \frac{f_e(\tilde{\mathbf{p}}, \bar{\mathbf{q}})}{x_e^{(k)} g_e(\tilde{\mathbf{p}}, \bar{\mathbf{q}})}. \qquad (15)$$

Note that the problem (15) is a fractional programming that can be solved efficiently by employing Dinkelbach's method [36] given in **Algorithm 2**, as follows:

$$(\tilde{\mathbf{p}}_i^*, \bar{\mathbf{q}}_i^*) = \underset{\tilde{\mathbf{p}}, \bar{\mathbf{q}} \in \mathcal{P}}{\arg\max} \ \chi \qquad (16a)$$
$$\text{s.t.} \quad f_e(\tilde{\mathbf{p}}, \bar{\mathbf{q}}) - \gamma_i x_e^{(k)} g_e(\tilde{\mathbf{p}}, \bar{\mathbf{q}}) \geq \chi, \ \forall e, \qquad (16b)$$

where χ is an auxiliary variable and γ_i is the Dinkelbach parameter. The problem (16) can be solved efficiently by applying convex optimization solvers such as CVX [38]. The flowchart of for this optimal solution is shown in Fig. 3.

Algorithm 1 Outer Polyblock Approximation Algorithm

1: **Initialize**
   Set the iterations index $i = 1$ and the maximum tolerance $\epsilon \ll 1$. Set $u_{m,k}^n = 1 + g_m^n P_{\max,\text{CU}}$ and $v_{k,m}^n = 1 + h_k^n P_{\max,\text{DU}}$ to build the polyblock $\mathcal{B}^{(1)}$ with vertex set $\mathcal{H}^{(1)} = \{\mathbf{x}^{(1)}\}$.
2: **repeat** {Main Loop}
3: Build a smaller polyblock $\mathcal{B}^{(i+1)}$ with vertex set $\mathcal{H}^{(i+1)}$ by substituting $\mathbf{x}^{(i)}$ with new vertices $\{\tilde{\mathbf{x}}_1^{(i)}, \tilde{\mathbf{x}}_2^{(i)}, \ldots, \tilde{\mathbf{x}}_{\mathcal{E}}^{(i)}\}$ where $\tilde{\mathbf{x}}_e^{(i)}$ can be obtained by $\tilde{\mathbf{x}}_e^{(1)} = \mathbf{x}^{(1)} - (x_e^{(1)} - \phi(\mathbf{x}^{(1)}))\mathbf{v}_e$. In particular, the e-th element of $\Phi(\mathbf{x}^{(i)})$ is $\phi(\mathbf{x}^{(i)})$ which can be obtained by Algorithm 2.
4: Find the new vertex $\mathbf{x}^{(i+1)}$ by solving the following maximization problem
   $$\mathbf{x}^{(i+1)} = \underset{\mathbf{x} \in \mathcal{H}^{(i+1)} \cap \mathcal{G}}{\arg\max} \left\{ \sum_{j=1}^{\mathcal{E}} \log_2(\phi_j(\mathbf{x})^{\mu_j}) \right\}.$$
5: Set $i = i + 1$.
6: **until** $\frac{\|\mathbf{x}^{(i)} - \phi(\mathbf{x}^{(i)})\|}{\|\mathbf{x}^{(i)}\|} \leq \epsilon$
7: **Return** $\mathbf{x}^* = \Phi(\mathbf{x}^{(i)})$, $\tilde{\mathbf{p}}_i^*$, and $\bar{\mathbf{q}}_i^*$

Algorithm 2 Projection Algorithm

1: **Initialize**
   Set the iteration index $d = 1$ and the maximum tolerance $\delta \ll 1$, and initialize $\gamma_j = 0$.
2: **repeat** {Main Loop}
3: $(\tilde{\mathbf{p}}_d^*, \bar{\mathbf{q}}_d^*) = \underset{\tilde{\mathbf{p}}, \bar{\mathbf{q}} \in \mathcal{P}}{\arg\max} \min_{1 \leq e \leq \mathcal{E}} \{f_e(\tilde{\mathbf{p}}, \bar{\mathbf{q}}) - \gamma_j x_e^{(k)} g_e(\tilde{\mathbf{p}}, \bar{\mathbf{q}})\}$.
4: $\gamma_{d+1} = \min_{1 \leq e \leq \mathcal{E}} \frac{f_e(\tilde{\mathbf{p}}, \bar{\mathbf{q}})}{x_e^{(k)} g_e(\tilde{\mathbf{p}}, \bar{\mathbf{q}})}$.
5: Set $d = d + 1$
6: **until** $\min_{1 \leq e \leq \mathcal{E}} \{f_e(\tilde{\mathbf{p}}^*_{d-1}, \bar{\mathbf{q}}^*_{d-1}) - \gamma_j x_e^{(k)} g_e(\tilde{\mathbf{p}}^*_{d-1}, \bar{\mathbf{q}}^*_{d-1})\} \leq \delta$
7: **Return** $\Phi(\mathbf{x}^{(k)}) = \gamma_j \mathbf{x}^{(k)}$, $\tilde{\mathbf{p}}^*_{d-1}$, and $\bar{\mathbf{q}}^*_{d-1}$

Additionally, the optimal subchannel allocation policies φ_k^n and ψ_m^n can be obtained as:

$$\varphi_k^{*n}, \psi_m^{*n} = \begin{cases} 1 & u_{m,k}^n > 1, \ v_{k,m}^n > 1, \\ 0 & otherwise. \end{cases} \qquad (17)$$

As a result, the proposed monotonic method to solve the problem (10a) can obtain the globally optimal solution [32]. However, it can be perceived that the computational complexity of monotonic approach is too high and grows exponentially with the number of vertices, applied in each iteration.

In what follows, we provide a suboptimal resource allocation algorithm with much lower complexity than that of monotonic approach to make a tradeoff between complexity and performance gain.

B. SUBOPTIMAL SOLUTION

In this subsection, we propose a low-complexity suboptimal algorithm based on SCA that provides a locally optimal solution for the optimization problem in (7). To solve the highly non-convex optimization problem (10), we apply an approach
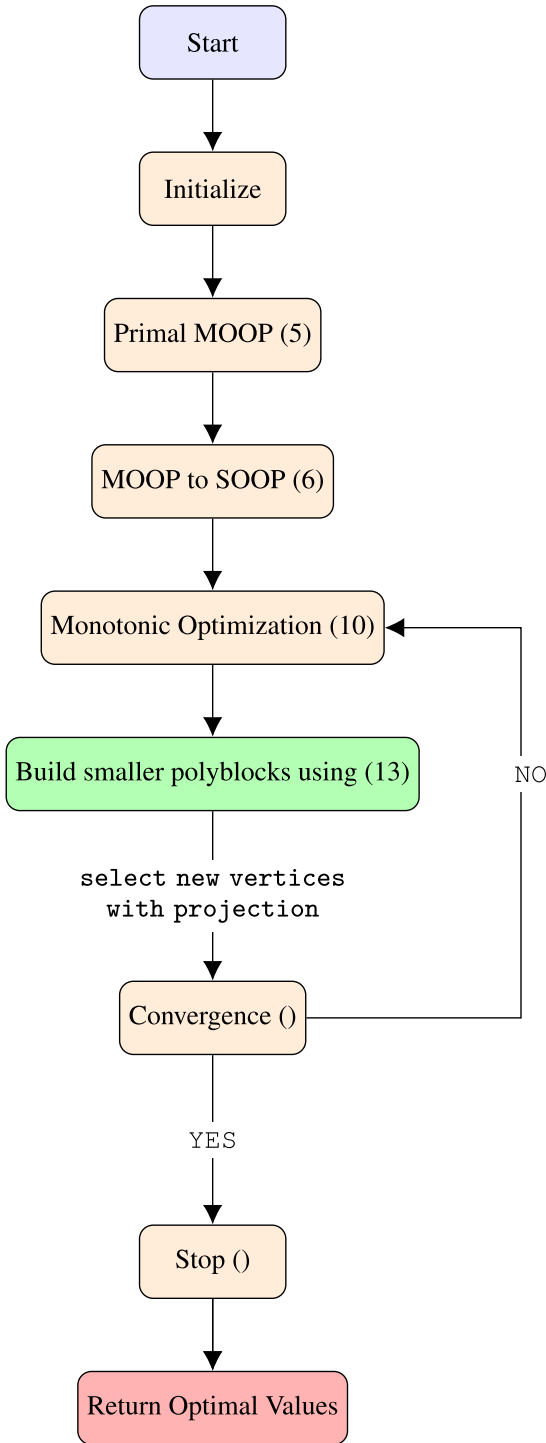
FIGURE 3. Flowchart of the optimal solution.

that deals with subchannel assignment and power allocation as follows.

The product terms $\varphi_k^n p_k^n$ and $\psi_m^n \hat{p}_m^n$ are the main obstacles for the design of an efficient resource allocation algorithm due to the binary nature of φ_k^n and ψ_m^n. To tackle this issue, we impose two additional constraints to convert optimization

variables φ_k^n and ψ_m^n into continuous variables as:

$$\ddot{C}_1 : 0 \leq p_k^n \leq \varphi_k^n P_{\max,\text{DU}}, \quad \forall n, k, \tag{18}$$

$$\ddot{C}_2 : 0 \leq \hat{p}_m^n \leq \psi_m^n P_{\max,\text{CU}}, \quad \forall n \in \mathcal{N}, m \in \mathcal{M}. \tag{19}$$

We remove φ_k^n and ψ_m^n from (10) while adding (18) and (19) in (10). Following [23], we relax the binary variable φ_k^n in C_6(5j) as:

$$\ddot{C}_3 : \sum_{k=1}^{K} \sum_{n=1}^{N} \varphi_k^n - \sum_{k=1}^{K} \sum_{n=1}^{N} \left(\varphi_k^n\right)^2 \leq 0, \tag{20}$$

$$\ddot{C}_4 : 0 \leq \varphi_k^n \leq 1, \quad \forall n \in \mathcal{N}, k \in \mathcal{K}, \tag{21}$$

and similarly constraining on the binary variable ψ_m^n in C_7(5k) can be stated as:

$$\ddot{C}_5 : \sum_{m=1}^{M} \sum_{n=1}^{N} \psi_m^n - \sum_{m=1}^{M} \sum_{n=1}^{N} \left(\psi_m^n\right)^2 \leq 0, \tag{22}$$

$$\ddot{C}_6 : 0 \leq \psi_m^n \leq 1, \quad \forall n \in \mathcal{N}, m \in \mathcal{M}. \tag{23}$$

Now, the optimization variables φ_k^n and ψ_m^n are continuous values between 0 and 1. In order to handle constraints $\ddot{C}_3$(20) and $\ddot{C}_4$(22), we reformulate the problem in (10) as:

$$\max_{\{\mathbf{p},\hat{\mathbf{p}},\boldsymbol{\varphi},\boldsymbol{\psi}\}} \mathcal{W}(\mathbf{p}, \hat{\mathbf{p}}, \boldsymbol{\varphi}, \boldsymbol{\psi})$$

$$- \lambda_\varphi \left(\sum_{k=1}^{K} \sum_{n=1}^{N} \varphi_k^n - \sum_{k=1}^{K} \sum_{n=1}^{N} \left(\varphi_k^n\right)^2 \right)$$

$$- \lambda_\psi \left(\sum_{m=1}^{M} \sum_{n=1}^{N} \psi_m^n - \sum_{m=1}^{M} \sum_{n=1}^{N} \left(\psi_m^n\right)^2 \right)$$

$$\text{s.t. } C_1(5e) - C_4(5h), \ \ddot{C}_1(18) - \ddot{C}_2(19), \ \ddot{C}_4(21),$$

$$\text{and } \ddot{C}_6(23), \tag{24}$$

where λ_φ and λ_ψ are large penalty factors to penalize the objective function for any φ_k^n and ψ_m^n, respectively, that are not equal to 0 or 1, i.e., large penalty terms in the objective function (24) enforce φ_k^n and ψ_m^n to be 0 or 1. It can be shown that with an appropriate choice of λ_φ and λ_ψ, problems (5) and (24) are equivalent in the sense that they result into the same optimal solution [17], [23], [24], [33]. Now, we change (24) as:

$$\max_{\{\mathbf{p},\hat{\mathbf{p}},\boldsymbol{\varphi},\boldsymbol{\psi}\}} A\left(\mathbf{p}, \hat{\mathbf{p}}, \boldsymbol{\varphi}, \boldsymbol{\psi}\right) - B\left(\mathbf{p}, \hat{\mathbf{p}}, \boldsymbol{\varphi}, \boldsymbol{\psi}\right)$$

$$\text{s.t. } C_1(5e) - C_4(5h), \ \ddot{C}_1(18) - \ddot{C}_2(19),$$

$$\ddot{C}_4(21), \text{ and } \ddot{C}_6(23),$$

$$a(\mathbf{p}, \hat{\mathbf{p}}) - b(\mathbf{p}, \hat{\mathbf{p}}) \geq R_{\min,m,\text{CU}},$$

$$c(\mathbf{p}, \hat{\mathbf{p}}) - d(\mathbf{p}, \hat{\mathbf{p}}) \geq R_{\min,k,\text{DU}}, \tag{25}$$

where $A(\mathbf{p}, \hat{\mathbf{p}}, \boldsymbol{\varphi}, \boldsymbol{\psi})$, $B(\mathbf{p}, \hat{\mathbf{p}}, \boldsymbol{\varphi}, \boldsymbol{\psi})$, $a(\mathbf{p},\hat{\mathbf{p}})$, $b(\mathbf{p}, \hat{\mathbf{p}})$, $c(\mathbf{p}, \hat{\mathbf{p}})$, and $d(\mathbf{p}, \hat{\mathbf{p}})$ are defined at the top of the next pages respectively in formulas (26)-(31). It can be see that $A\left(\mathbf{p}, \hat{\mathbf{p}}, \boldsymbol{\varphi}, \boldsymbol{\psi}\right)$ and $B\left(\mathbf{p}, \hat{\mathbf{p}}, \boldsymbol{\varphi}, \boldsymbol{\psi}\right)$ are two concave functions.

So, the optimization problem now belongs to the class of difference of convex (D.C.) function programming, where

successive convex approximation can be applied to obtain a locally optimal solution [17], [24]–[26], [34]. Since $B\left(\mathbf{p}, \hat{\mathbf{p}}, \boldsymbol{\varphi}, \boldsymbol{\psi}\right)$, $b(\mathbf{p}, \hat{\mathbf{p}})$, and $d(\mathbf{p}, \hat{\mathbf{p}})$ are differentiable convex functions, we employ the first-order Taylor approximation for $B\left(\mathbf{p}, \hat{\mathbf{p}}, \boldsymbol{\varphi}, \boldsymbol{\psi}\right)$, $b(\mathbf{p}, \hat{\mathbf{p}})$, and $d(\mathbf{p}, \hat{\mathbf{p}})$ at the t-th iteration to make a convex optimization as:

$$
\begin{aligned}
\tilde{B}&\left(\mathbf{p}, \hat{\mathbf{p}}, \boldsymbol{\varphi}, \boldsymbol{\psi}\right) \\
&\simeq B\big(\mathbf{p}^{t-1}, \hat{\mathbf{p}}^{t-1}, \boldsymbol{\varphi}^{t-1}, \boldsymbol{\psi}^{t-1}\big) \\
&\quad + \nabla_{\mathbf{p}} B\big(\mathbf{p}^{t-1}, \hat{\mathbf{p}}^{t-1}, \boldsymbol{\varphi}^{t-1}, \boldsymbol{\psi}^{t-1}\big).\big(\mathbf{p} - \mathbf{p}^{t-1}\big) \\
&\quad + \nabla_{\hat{\mathbf{p}}} B\big(\mathbf{p}^{t-1}, \hat{\mathbf{p}}^{t-1}, \boldsymbol{\varphi}^{t-1}, \boldsymbol{\psi}^{t-1}\big).\big(\hat{\mathbf{p}} - \hat{\mathbf{p}}^{t-1}\big) \\
&\quad + \nabla_{\boldsymbol{\varphi}} B\big(\mathbf{p}^{t-1}, \hat{\mathbf{p}}^{t-1}, \boldsymbol{\varphi}^{t-1}, \boldsymbol{\psi}^{t-1}\big).\big(\boldsymbol{\varphi} - \boldsymbol{\varphi}^{t-1}\big) \\
&\quad + \nabla_{\boldsymbol{\psi}} B\big(\mathbf{p}^{t-1}, \hat{\mathbf{p}}^{t-1}, \boldsymbol{\varphi}^{t-1}, \boldsymbol{\psi}^{t-1}\big).\big(\boldsymbol{\psi} - \boldsymbol{\psi}^{t-1}\big),
\end{aligned}
\tag{32}
$$

$$
\begin{aligned}
\tilde{b}\left(\mathbf{p}, \hat{\mathbf{p}}\right) &\simeq b\left(\mathbf{p}^{t-1}, \hat{\mathbf{p}}^{t-1}\right) \\
&\quad + \nabla_{\mathbf{p}} b\left(\mathbf{p}^{t-1}, \hat{\mathbf{p}}^{t-1}\right).\left(\mathbf{p} - \mathbf{p}^{t-1}\right) \\
&\quad + \nabla_{\hat{\mathbf{p}}} b\left(\mathbf{p}^{t-1}, \hat{\mathbf{p}}^{t-1}\right).\left(\hat{\mathbf{p}} - \hat{\mathbf{p}}^{t-1}\right),
\end{aligned}
\tag{33}
$$

$$
\begin{aligned}
\tilde{d}\left(\mathbf{p}, \hat{\mathbf{p}}\right) &\simeq d\left(\mathbf{p}^{t-1}, \hat{\mathbf{p}}^{t-1}\right) \\
&\quad + \nabla_{\mathbf{p}} d\left(\mathbf{p}^{t-1}, \hat{\mathbf{p}}^{t-1}\right).\left(\mathbf{p} - \mathbf{p}^{t-1}\right)
\end{aligned}
$$

$$
+ \nabla_{\hat{\mathbf{p}}} d\left(\mathbf{p}^{t-1}, \hat{\mathbf{p}}^{t-1}\right).\left(\hat{\mathbf{p}} - \hat{\mathbf{p}}^{t-1}\right).
\tag{34}
$$

Since $B\left(\mathbf{p}, \hat{\mathbf{p}}, \boldsymbol{\varphi}, \boldsymbol{\psi}\right)$ $b\left(\mathbf{p}^{t-1}, \hat{\mathbf{p}}^{t-1}\right)$, and $d\left(\mathbf{p}^{t-1}, \hat{\mathbf{p}}^{t-1}\right)$ are concave functions, the gradient are also supergradient. Therefore, we have the following inequality:

$$
B\left(\mathbf{p}, \hat{\mathbf{p}}, \boldsymbol{\varphi}, \boldsymbol{\psi}\right) \leq \tilde{B}\left(\mathbf{p}, \hat{\mathbf{p}}, \boldsymbol{\varphi}, \boldsymbol{\psi}\right),
\tag{35}
$$

$$
b\left(\mathbf{p}^{t-1}, \hat{\mathbf{p}}^{t-1}\right) \leq \tilde{b}\left(\mathbf{p}^{t-1}, \hat{\mathbf{p}}^{t-1}\right),
\tag{36}
$$

$$
d\left(\mathbf{p}^{t-1}, \hat{\mathbf{p}}^{t-1}\right) \leq \tilde{d}\left(\mathbf{p}^{t-1}, \hat{\mathbf{p}}^{t-1}\right).
\tag{37}
$$

In a similar manner, we can handle the minimum data-rate requirement to make a convex constraint. In fact, we adopt the first-order Taylor approximation for $b(\mathbf{p}, \hat{\mathbf{p}})$ and $d(\mathbf{p}, \hat{\mathbf{p}})$ respectively to obtain a convex constraint. Therefore, a lower bound for any given $\mathbf{p}^{t-1}, \hat{\mathbf{p}}^{t-1}, \boldsymbol{\varphi}^{t-1}$ and $\boldsymbol{\psi}^{t-1}$ can be found by solving the following convex optimization problem:

$$
\begin{aligned}
\max_{\{\mathbf{p}, \hat{\mathbf{p}}, \boldsymbol{\varphi}, \boldsymbol{\psi}\}} \quad & A\left(\mathbf{p}, \hat{\mathbf{p}}, \boldsymbol{\varphi}, \boldsymbol{\psi}\right) - \tilde{B}\left(\mathbf{p}, \hat{\mathbf{p}}, \boldsymbol{\varphi}, \boldsymbol{\psi}\right) \\
\text{s.t. } & C_1(5\mathrm{e}) - C_4(5\mathrm{h}),\ \ddot{C}_1(18) - \ddot{C}_2(19), \\
& \ddot{C}_4(21),\ \text{and } \ddot{C}_6(23), \\
& a(\mathbf{p}, \hat{\mathbf{p}}) - \tilde{b}(\mathbf{p}, \hat{\mathbf{p}}) \geq R_{\min,m,\mathrm{CU}}, \\
& c(\mathbf{p}, \hat{\mathbf{p}}) - \tilde{d}(\mathbf{p}, \hat{\mathbf{p}}) \geq R_{\min,k,\mathrm{DU}}.
\end{aligned}
\tag{38}
$$

$$
\begin{aligned}
A(\mathbf{p}, \hat{\mathbf{p}}, \boldsymbol{\varphi}, \boldsymbol{\psi}) ={}& \frac{\beta}{\omega_\beta}\left(\sum_{m=1}^{M}\sum_{n=1}^{N}\log_2\left(\hat{p}_m^n g_m^n + N_0 B_c + \sum_{k=1}^{K} p_k^n \hat{h}_k^{\prime n}\right)\right) \\
&+ \frac{\alpha}{\omega_\alpha}\left(\sum_{k=1}^{K}\sum_{n=1}^{N}\log_2\left(p_k^n h_k^n + N_0 B_c + \sum_{m=1}^{M}\hat{p}_m^n g_m^{\prime n} + \sum_{\substack{k'=1, \\ k'\neq k}}^{K} p_{k'}^n \hat{h}_{k',k}^{\prime n}\right)\right) \\
&- \frac{\gamma}{\omega_\gamma}\left(\sum_{k=1}^{K}\sum_{n=1}^{N} p_k^n\right) - \frac{\delta}{\omega_\delta}\left(\sum_{m=1}^{M}\sum_{n=1}^{N}\hat{p}_m^n\right) - \lambda_\varphi\left(\sum_{k=1}^{K}\sum_{n=1}^{N}\varphi_k^n\right) - \lambda_\psi\left(\sum_{m=1}^{M}\sum_{n=1}^{N}\psi_m^n\right),
\end{aligned}
\tag{26}
$$

$$
\begin{aligned}
B(\mathbf{p}, \hat{\mathbf{p}}, \boldsymbol{\varphi}, \boldsymbol{\psi}) ={}& \frac{\beta}{\omega_\beta}\left(\sum_{m=1}^{M}\sum_{n=1}^{N}\log_2\left(N_0 B_c + \sum_{k=1}^{K} p_k^n \hat{h}_k^{\prime n}\right)\right) \\
&+ \frac{\alpha}{\omega_\alpha}\left(\sum_{k=1}^{K}\sum_{n=1}^{N}\log_2\left(N_0 B_c + \sum_{m=1}^{M}\hat{p}_m^n g_m^{\prime n} + \sum_{\substack{k'=1, \\ k'\neq k}}^{K} p_{k'}^n \hat{h}_{k',k}^{\prime n}\right)\right) \\
&- \lambda_\varphi\left(\sum_{k=1}^{K}\sum_{n=1}^{N}(\varphi_k^n)^2\right) - \lambda_\psi\left(\sum_{m=1}^{M}\sum_{n=1}^{N}(\psi_m^n)^2\right).
\end{aligned}
\tag{27}
$$

$$
a(\mathbf{p}, \hat{\mathbf{p}}) = \sum_{n=1}^{N}\log_2\left(\hat{p}_m^n g_m^n + N_0 B_c + \sum_{k=1}^{K} p_k^n \hat{h}_k^{\prime n}\right)
\tag{28}
$$

$$
b(\mathbf{p}, \hat{\mathbf{p}}) = \sum_{n=1}^{N}\log_2\left(N_0 B_c + \sum_{k=1}^{K} p_k^n \hat{h}_k^{\prime n}\right)
\tag{29}
$$

$$
c(\mathbf{p}, \hat{\mathbf{p}}) = \sum_{n=1}^{N}\log_2\left(p_k^n h_k^n + N_0 B_c + \sum_{m=1}^{M}\hat{p}_m^n g_m^{\prime n} + \sum_{k'\neq k}^{K}\varphi_{k'}^n p_k^n \hat{h}_{k',k}^{\prime n}\right)
\tag{30}
$$

$$
d(\mathbf{p}, \hat{\mathbf{p}}) = \sum_{n=1}^{N}\log_2\left(N_0 B_c + \sum_{m=1}^{M}\hat{p}_m^n g_m^{\prime n} + \sum_{k'\neq k}^{K}\varphi_{k'}^n p_k^n \hat{h}_{k',k}^{\prime n}\right)
\tag{31}
$$

Algorithm 3 Proposed Method Based on D.C. Programming

1: **Initialize**
   Set $t = 0$, maximum number of iterations T_{max}, penalty factors $\lambda_\varphi, \lambda_\psi \gg 1$, set appropriate weighting coefficients factors and set feasible vectors $\mathbf{p}^0, \hat{\mathbf{p}}^0, \boldsymbol{\varphi}^0$, and $\boldsymbol{\psi}^0$.
2: **repeat** {Main Loop}
3:   Update $\tilde{B}(\mathbf{p}, \hat{\mathbf{p}}, \boldsymbol{\varphi}, \boldsymbol{\psi})$ as presented in (32).
4:   Solve optimization problem of (38) and store the intermediate resource allocation policy $\mathbf{p}, \hat{\mathbf{p}}, \boldsymbol{\varphi}$, and $\boldsymbol{\psi}$
5:     Set $t = t + 1$.
6:     Set $\mathbf{p}^t = \mathbf{p}$, $\hat{\mathbf{p}}^t = \hat{\mathbf{p}}$, $\boldsymbol{\varphi}^t = \boldsymbol{\varphi}$, and $\boldsymbol{\psi}^t = \boldsymbol{\psi}$.
7: **until** convergence or $t = T_{max}$
8: **Return** $\mathbf{p}^*, \hat{\mathbf{p}}^*, \boldsymbol{\varphi}^*, \boldsymbol{\psi}^*$

The iterative algorithm shown in **Algorithm 3** is employed to achieve a lower bound. In fact, this iterative algorithm can be adopted to tighten the obtained lower bound where the solution of (38) in iteration (t) is exploited as an initial point for the next iteration $(t + 1)$. It should be noted that the sub-optimal iterative algorithm reaches a locally optimal solution of the original problem (5) with a polynomial time complexity [17], [24]–[26], [33]–[35]. The flowchart of this suboptimal solution is depicted in Fig. 4.

V. COMPUTATIONAL COMPLEXITY

In this section, the computational complexity of the proposed algorithm is provided, which mainly is influenced by the configuration of the objective function and the constraints that create the normal set. Notably, the polyblock algorithm comprises the subsequent stages. In the first stage, the most suitable vertex by its projection on the normal set is determined. Subsequently, the projection of the picked vertex is obtained. Eventually, we obtained the new vertex set by eliminating the inappropriate vertices. In particular, the dimension of problem, the number of iterations required for convergence, and the number of iterations expected for the projection of each vertex are assumed to be L_1, L_2 and L_3, respectively. In summary, the complexity order of monotonic approach can be stated as $\mathcal{O}(L_2(L_2 \times L_1 + L_3))$ [26], [31]. For the sub-optimal solution the optimization problem (38) includes $(2NK + 2NM)$ decision variables while consists of $K + M + M + K + N + N + NK + NM$ convex and linear constraints. Hence, its computational complexity is the order of $\mathcal{O}(2NK + 2NM)^3(2M + 2K + 2N + KN + NM)$. It can be concluded that the computational complexity asymptotically is in the order of $\mathcal{O}(NK + NM)^4$, which shows the polynomial time complexity.

VI. NUMERICAL RESULTS

In this section, we evaluate the performance of the proposed resource allocation algorithms for D2D underlaying cellular networks in uplink OFDMA communications via extensive simulations. There is a single macro cell in which the diameter is set to 250 meters. In this cell, there are two CUs and two
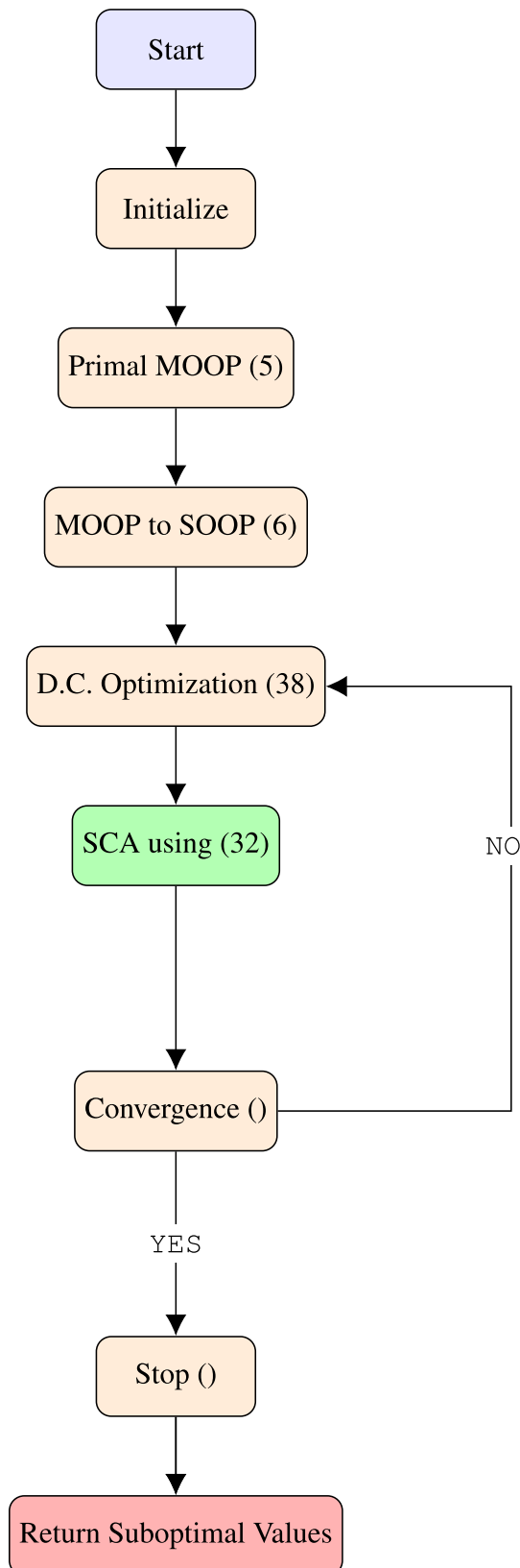
FIGURE 4. Flowchart of the suboptimal solution.

DUs, i.e., $M = K = 2$. We also study a frequency-selective fading channel and further assume the central carrier frequency of 3 GHz. The number of subcarriers is $N = 8$,

where each subcarrier's bandwidth is equal to 180 kHz. The power of the background noise is N_0 = -120 dBm in all simulations. We assume that each subchannel experiences Rayleigh flat fading, which includes the path-loss model for CUs as $128.1 + 37.6 \log(d)$, and $148.1 + 40 \log(d)$ DUs, where d is the distance (in km). Moreover, considering a line-of-sight (LoS) signal in the received signal, the small-scale fading channel is modeled as Rician fading with Rician factor $\rho = 3$ dB. These parameters for propagation modeling and simulations obey the recommendations in 3GPP evaluation methodology [40]. For the power consumption model, a constant consumed circuit power, P_{c_m}, equall to 23 dBm is considered for CUs. Besides, a constant power consumption of 20 dBm is assumed for each DU, i.e., $P_{c_k} = 20$ dBm. The maximum power budgets of both DUs and CUs are assumed to be equal, i.e., $P_{\max,\mathrm{CU}} = P_{\max,\mathrm{DU}} = 25$ dBm. The target transmission data-rates for both CUs and DUs are set to $R_{\min,k,\mathrm{CU}} = R_{\min,m,\mathrm{DU}} = 1$ bits/sec/Hz (bps/Hz). Note that all figures shown in this section are obtained by calculating the average over different realizations of path loss as well as multi-path fading. These simulation parameters are enlisted in **Table 1** unless otherwise is specified.

TABLE 1. Simulation parameters.

Parameter	Value
Cell diameter	250 m
Distance between D2D link	30m
Number of CUs (M)	2
Number of DUs (K)	2
Number of sub-carriers (N)	8
Noise power (N_0)	-120 dBm
Sub-carrier bandwidth	180 kHz
Path-loss model for CUs	$128.1 + 37.6 \log(d)$
Path-loss model for DUs	$148.1 + 40 \log(d)$
Small scale fading distribution	Rician fading with factor 3 dB
Power consumed by the kth CU (P_{c_m})	23 dBm
Power consumed by the kth DU (P_{c_k})	20 dBm
Maximum transmit power of the CUs	25 dBm
Maximum transmit power of the DUs	25 dBm
Minimum data-rate for CUs ($R_{\min,\mathrm{CU}}$)	1 bps/Hz
Minimum data-rate for DUs ($R_{\min,\mathrm{DU}}$)	1 bps/Hz
Channel realization number	100

A. AVERAGE SUM RATE VS. WEIGHT

Fig. 5 shows the sum rates of cellular and D2D networks for different (fixed) values for γ and δ with $\gamma + \delta = 0.2$ when α is changing from 0 to 0.8 (equivalently β is varied from $0.8 - \alpha$ to 0). From this figure, we observe that as α increases, the sum rate of D2D links increases while the sum rate of the cellular links starts to decline. This is because when α increases, the importance of the maximization of the D2D rate increases, which results in an increase of the sum rate of the DUs. Moreover, this figure illustrates the maximum sum rate for different values of γ and δ. It is observed that when the weight γ for power minimization of the DUs increases, the sum rate of the DUs tends to increase. However, the value of α for which the maximum sum rate is obtained, varies from one case to another. Furthermore, Fig. 5 shows that the

proposed suboptimal scheme closely approaches the optimal solution.

Fig. 6 compares the total rate of both DUs and CUs versus α for the MOOP in (10a), when α changes from 0 to 1 (equivalently β varies from $1 - \alpha$ to 0) with fixed values of $\gamma = \delta = 0$, and the rate for the algorithm proposed in [2], when $\alpha = 1$ with fixed values of $\beta = \gamma = \delta = 0$. From Fig. 6, it can be concluded that the total rate of both DUs and CUs obtained with the MOOP (10a) is higher than the total rate of both DUs and CUs in [2] for $0 < \alpha < 0.9$, which shows the efficacy of the proposed formulation. This is because the algorithm from [2], which only maximizes the total rate of the DUs, does not use the capability of the whole network. Another important observation in Fig. 6 is the superiority of the proposed algorithm for certain values of α, in our setting $0.4 \leq \alpha \leq 0.7$, compared to the SOOP with the objective function $R_{\mathrm{DU}} + R_{\mathrm{CU}}$. Note that as α gets closer to its optimal value (in peaks), the total system throughput achieved using MOOP becomes higher than SOOP. This is due to the fact that via the MOOP approach, more degrees of freedom can be exploited to enhance the data-rate of the network. Outside the interval $0.4 < \alpha < 0.7$, the weighting factor makes either R_{DU} or R_{CU} dominant in the expression (13), making the other rate subordinated to the other, implying the dominated rate will be negligibly small, while the other rate only slightly increases. On the contrary, in the SOOP formulation, the weights for R_{DU} and R_{CU} are equal, leading to an identical resource allocation policy for both DUs and CUs. Finally, Fig. 6 also proves that the proposed suboptimal scheme closely follows the optimal solution.
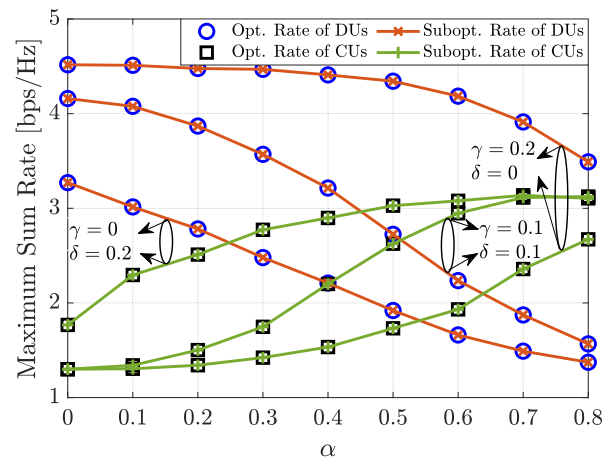

FIGURE 5. Maximum sum rate of D2D and cellular networks vs. α.

B. RATE-POWER REGION

Fig. 7 and Fig. 8 investigate the total power consumption versus the minimum data rate requirement and total data-rate of the system, respectively, for both the optimal and suboptimal algorithms. In order to plot these rate-power region figures,
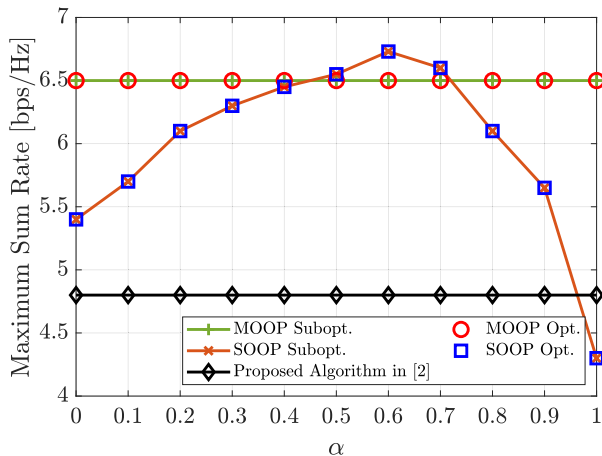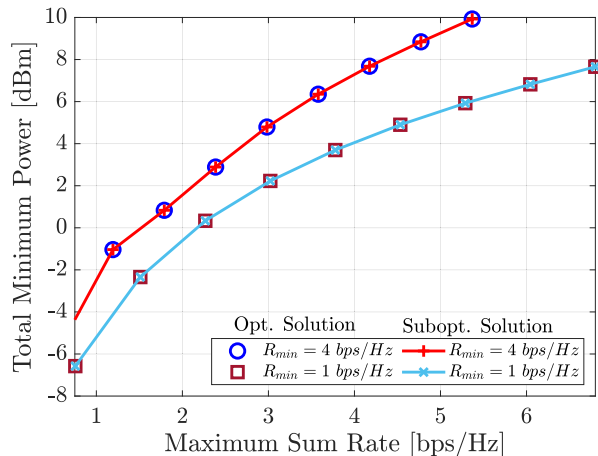
FIGURE 6. Comparing MOOP with SOOP.

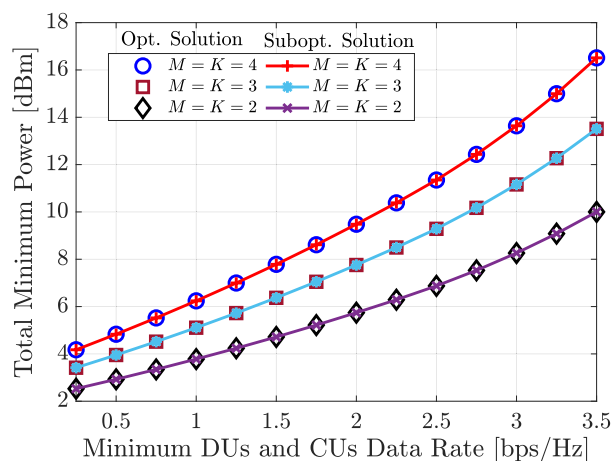**FIGURE 8.** Rate-power region.

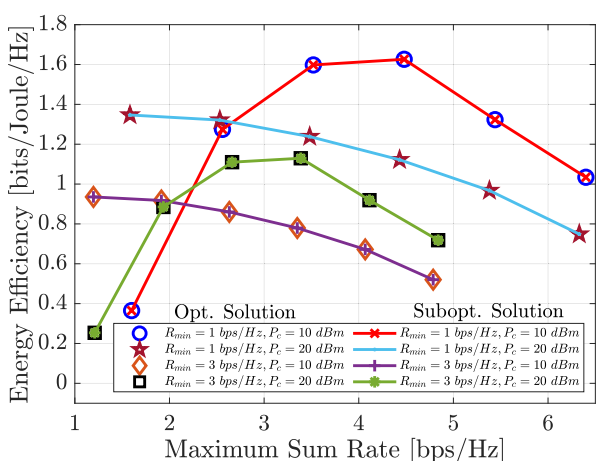**FIGURE 7.** Minimum total power vs minimum data-rate of both CUs and DUs.

FIGURE 9. Maximum sum data-rate vs. EE.

we define the following optimization problem:

$$\max_{\{\mathbf{p},\hat{\mathbf{p}},\boldsymbol{\varphi},\boldsymbol{\psi}\}} \overline{R}_{tot} = R_{DU} + R_{CU}, \tag{39a}$$

$$\min_{\{\mathbf{p},\hat{\mathbf{p}},\boldsymbol{\varphi},\boldsymbol{\psi}\}} \overline{P}_{tot} = P_{DU} + P_{CU}, \tag{39b}$$

$$\text{s.t. } C_1(5e) - C_7(5k). \tag{39c}$$

Using a similar method as in (6), (39) can be stated as:

$$\max_{\{\mathbf{p},\hat{\mathbf{p}},\boldsymbol{\varphi},\boldsymbol{\psi}\}} \frac{\hat{\alpha}}{\omega_{\hat{\alpha}}} \overline{R}_{tot} - \frac{\hat{\beta}}{\omega_{\hat{\beta}}} \overline{P}_{tot} \tag{40a}$$

$$\text{s.t. } C_1(5e) - C_7(5k), \tag{40b}$$

where, $\hat{\alpha} + \hat{\beta} = 1$. In particular, we set $\alpha + \beta = \hat{\alpha}$ and $\delta + \gamma = \hat{\beta}$ in (6).

For plotting Fig. 7, we set the value of $\hat{\alpha}$ equal to zero, and view the power consumption versus the minimum data rate of users. The tradeoff between the total minimum power and the maximum data rate is shown in Fig. 7 for a different number of CUs and DUs. We can also observe that by increasing the number of users in the network, the total minimum power

increases for a given minimum user data-rate. Moreover, when the value of the minimum data rate increases, a minimum power value increases as well. This is because more transmit power is required to meet the minimum data rate, which leads to an increase of the transmit power.

Fig. 8 illustrates the region of the total minimum power versus the total rate for the different value of $R_{\min}$. The tradeoff region in this figure is obtained by solving the problem (40) via changing the values of $0 \leq \hat{\alpha} \leq 1$, with a step size 0.1. It can be seen that the total minimum power is a monotonically increasing function with respect to the maximum sum data-rate. This result confirms that total power minimization and total rate maximization are conflicting system design objectives in general. The figure also shows that for a lower value of $R_{\min}$, less minimum power can be expected. Lastly, as can be observed, the suboptimal low-complexity solution tends to be closely following the optimal solution.

C. RATE-ENERGY TRADEOFF
Fig. 9 shows the tradeoff between EE and R_{tot} for different values of P_c and $R_{\min}$. This figure is achieved by changing

the weighting coefficient. Note that EE is defined as $\overline{\mathcal{EE}} = \frac{\overline{R}_{tot}}{\sum_{k \in \mathcal{K}} P_{c_k} + \sum_{m \in \mathcal{M}} P_{c_m} + \overline{P}_{tot}}$. Consequently, the EE optimization problem is formulated as follows:

$$\overline{\mathcal{EE}} = \frac{\overline{R}_{tot}}{\sum_{k \in \mathcal{K}} P_{c_k} + \sum_{m \in \mathcal{M}} P_{c_m} + \overline{P}_{tot}} \tag{41}$$

$$\text{s.t.} \quad C_1(5e) - C_7(5k). \tag{42}$$

In order to solve the $\overline{\mathcal{EE}}$, we define a new MOOP. In the new MOOP, the total data rate is maximized while the aggregated power consumption is minimized as follows:

$$\max_{\{\mathbf{p}, \hat{\mathbf{p}}, \varphi, \psi\}} \overline{R}_{tot} = R_{DU} + R_{CU}, \tag{43a}$$

$$\min_{\{\mathbf{p}, \hat{\mathbf{p}}, \varphi, \psi\}} \overline{P}_{tot} = P_{DU} + P_{CU}, \tag{43b}$$

$$\text{s.t.} \quad C_1(5e) - C_7(5k). \tag{43c}$$

Lemma 1: The solution of the MOOP (43) includes the solution of the SOOP EE-maximization (41).

Proof: Please see Appendix A.

For different values of R_{min} and $P_{c_k} = P_{c_m} = P_c = 20$ dBm, a bell-shaped curve is observed. The reason behind this is as follows. By increasing R_{tot}, the EE first increases to reach a maximum and then tends to decline. To have higher values of R_{tot}, the users need to transmit more power. While increasing the power, the gain of R_{tot} in the EE's numerator is smaller than the increase of the power in the EE denominator. This results in a reduction of the EE. For $P_{c_k} = P_{c_m} = P_c = 10$ dBm, EE decreases by increasing R_{tot}. This is because P_c is the dominant term. Furthermore, the EE is the ratio of total data rate to the total power, and the price to be paid for augments the total data rate is by far greater than the gain we attain because of the power consumed in the network.

VII. CONCLUSION

In this paper, to show the tradeoff between DUs and CUs in uplink OFDMA-based D2D communications, we presented a MOOP formulation that adjusts the power allocation strategy and subchannel assignment. The MOOP is converted to a SOOP using a weighted sum method and then solved via monotonic optimization to obtain an optimal solution. Furthermore, a suboptimal solution was proposed based on D.C. programming to compromise complexity and performance gain. While unveiling an interesting tradeoff region between total data-rate and total power consumption, the numerical results demonstrated the superiority of our proposed algorithm as compared to existing work addressed in the literature. Moreover, simulation results illustrated that more performance gain in the whole system could be achieved by the MOOP in which there is a cooperation between DUs and CUs. This leads to achieving the most appropriate allocated resources regarding different importance levels of networks. These observations are valid so far as the weights do not restrict the performance gain.

APPENDIX
PROOF OF LEMMA 1

To prove Lemma 1, we consider a general fractional programming formulated as follows:

$$\min_x \quad \phi(x) = \frac{f(x)}{g(x)} : x \in X, \tag{44}$$

where X is a nonempty compact set belonging to R^n. $f(x)$ and $g(x)$ denote continuous real-valued functions of $x \in X$ and $g(x) > 0$, for all $x \in X$. While addressing the optimal solution, let us define

$$\Gamma(\varphi) = \min \left\{ f(x) - \varphi^* g(x) : x \in X \right\}, \tag{45}$$

as the minimum value of $f(x) - \varphi g(x)$ for each fixed φ^*. According to Dinklebach's approach, it easily can be shown that

$$\varphi^* = \frac{f(x^*)}{g(x^*)} = \min_x \left\{ \frac{f(x)}{g(x)} : x \in X \right\}, \tag{46}$$

if and only if

$$\Gamma(\varphi^*) = \Gamma(\varphi^*, x^*)$$
$$= \min \left\{ f(x) - \varphi^* g(x) : x \in X \right\} = 0. \tag{47}$$

Hence, using (46) and (47), it is resulted that the optimal solution x^* of (44) is the optimal solution of (45) when $\varphi^* = \varphi$, where φ^* is the minimum value of (44).

Now, by formulating a general MOOP including two objectives we have

$$\min f(x) \tag{48a}$$

$$\max g(x) \tag{48b}$$

$$s.t. \, x > 0$$

where $f(x)$ and $g(x)$ can represent the numerator and denominator of fractional optimization problem in (44), respectively. We combine the competing objective functions (48a) and (48b) into a single objective function linearly through weighted-method, so the MOOP in (49) can be converted into a SOOP as:

$$\min \alpha f(x) - \beta g(x)$$
$$s.t. \, x > 0, \tag{49a}$$

where α and β are the weighting coefficients indicating the importance of the objectives. While comparing (49a) and (45), it can verify that optimal set of (49a) is inclusive of the solution for (45). ∎

REFERENCES

[1] A. Asadi, Q. Wang, and V. Mancuso, "A survey on device-to-device communication in cellular networks," *IEEE Commun. Surveys Tuts.*, vol. 16, no. 4, pp. 1801–1819, Nov. 2014.

[2] C. Kai, H. Li, L. Xu, Y. Li, and T. Jiang, "Joint subcarrier assignment with power allocation for sum rate maximization of D2D communications in wireless cellular networks," *IEEE Trans. Veh. Technol.*, vol. 68, no. 5, pp. 4748–4759, May 2019.

[3] R. Zhang, Y. Li, C.-X. Wang, Y. Ruan, Y. Fu, and H. Zhang, "Energy-spectral efficiency trade-off in underlaying mobile D2D communications: An economic efficiency perspective," *IEEE Trans. Wireless Commun.*, vol. 17, no. 7, pp. 4288–4301, Jul. 2018.

[4] K. Yang, S. Martin, C. Xing, J. Wu, and R. Fan, "Energy-efficient power control for device-to-device communications," *IEEE J. Sel. Areas Commun.*, vol. 34, no. 12, pp. 3208–3220, Dec. 2016.

[5] Q. Wu, G. Y. Li, W. Chen, and D. W. K. Ng, "Energy-efficient D2D overlaying communications with spectrum-power trading," *IEEE Trans. Wireless Commun.*, vol. 16, no. 7, pp. 4404–4419, Jul. 2017.

[6] T. D. Hoang, L. B. Le, and T. Le-Ngoc, "Energy-efficient resource allocation for D2D communications in cellular networks," *IEEE Trans. Veh. Technol.*, vol. 65, no. 9, pp. 6972–6986, Sep. 2016.

[7] Y. Sun, M. Peng, and H. V. Poor, "A distributed approach to improving spectral efficiency in uplink device-to-device-enabled cloud radio access networks," *IEEE Trans. Commun.*, vol. 66, no. 12, pp. 6511–6526, Dec. 2018.

[8] R. Yin, C. Zhong, G. Yu, Z. Zhang, K. K. Wong, and X. Chen, "Joint spectrum and power allocation for D2D communications underlaying cellular networks," *IEEE Trans. Veh. Technol.*, vol. 65, no. 4, pp. 2182–2195, Apr. 2016.

[9] Z. Kuang, G. Liu, G. Li, and X. Deng, "Energy efficient resource allocation algorithm in energy harvesting-based D2D heterogeneous networks," *IEEE Internet Things J.*, vol. 6, no. 1, pp. 557–567, Feb. 2019.

[10] Y. Wu, W. Liu, S. Wang, W. Guo, and X. Chu, "Network coding in device-to-device (D2D) communications underlaying cellular networks," in *Proc. IEEE Int. Conf. Commun. (ICC)*, Jun. 2015, pp. 2072–2077.

[11] S. Kim, "D2D enabled cellular network spectrum allocation scheme based on the cooperative bargaining solution," *IEEE Access*, vol. 8, pp. 53710–53719, 2020.

[12] C. Ma, Y. Li, H. Yu, X. Gan, X. Wang, Y. Ren, and J. J. Xu, "Cooperative spectrum sharing in D2D-enabled cellular networks," *IEEE Trans. Commun.*, vol. 64, no. 10, pp. 4394–4408, Oct. 2016.

[13] Y. Xiao, K.-C. Chen, C. Yuen, Z. Han, and L. A. DaSilva, "A Bayesian overlapping coalition formation game for device-to-device spectrum sharing in cellular networks," *IEEE Trans. Wireless Commun.*, vol. 14, no. 7, pp. 4034–4051, Jul. 2015.

[14] X. Lin, J. G. Andrews, and A. Ghosh, "Spectrum sharing for device-to-device communication in cellular networks," *IEEE Trans. Wireless Commun.*, vol. 13, no. 12, pp. 6727–6740, Dec. 2014.

[15] Y. Hao, Q. Ni, H. Li, and S. Hou, "Robust multi-objective optimization for EE-SE tradeoff in D2D communications underlaying heterogeneous networks," *IEEE Trans. Commun.*, vol. 66, no. 10, pp. 4936–4949, Oct. 2018.

[16] C. Vlachos and V. Friderikos, "MOCA: Multiobjective cell association for device-to-device communications," *IEEE Trans. Veh. Technol.*, vol. 66, no. 10, pp. 9313–9327, Oct. 2017.

[17] M. R. Mili, A. Khalili, D. W. K. Ng, and H. Steendam, "A novel performance tradeoff in heterogeneous networks: A multi-objective approach," *IEEE Wireless Commun. Letts.*, vol. 8, no. 5, pp. 1402–1405, Oct. 2019.

[18] M. R. Mili, A. Khalili, N. Mokari, S. Wittevrongel, D. W. K. Ng, and H. Steendam, "Tradeoff between ergodic energy efficiency and spectral efficiency in D2D communications under rician fading channel," *IEEE Trans. Veh. Technol.*, vol. 69, no. 9, pp. 9750–9766, Sep. 2020.

[19] S. Bayat, A. Khalili, S. Zargari, M. R. Mili, and Z. Han, "Multi-objective resource allocation for D2D and enabled MC-NOMA networks by tchebycheff method," *IEEE Trans. Veh. Technol.*, vol. 70, no. 5, pp. 4464–4470, May 2021.

[20] K. Miettinen, *Nonlinear Multiobjective Optimization*. Springer, 1999.

[21] J. Lee and S. Leyffer, *Mixed Integer Nonlinear Programming*. Springer, Dec. 2011.

[22] J. Jalali, "Resource allocation for SWIPT in multi-service wireless networks," M.S. thesis, Dept. Telecommun. Inf. Process., TELIN/IMEC, Ghent Univ., Ghent, Belgium, Jun. 2020. [Online]. Available: https://arxiv.org/abs/2007.13676

[23] A. Khalili, S. Akhlaghi, H. Tabassum, and D. W. K. Ng, "Joint user association and resource allocation in the uplink of heterogeneous networks," *IEEE Wireless Commun. Lett.*, vol. 9, no. 6, pp. 804–808, Jun. 2020.

[24] A. Khalili, M. R. Mili, M. Rasti, S. Parsaeefard, and D. W. K. Ng, "Antenna selection strategy for energy efficiency maximization in uplink OFDMA networks: A multi-objective approach," *IEEE Trans. Wireless Commun.*, vol. 19, no. 1, pp. 595–609, Jan. 2020.

[25] A. Khalili, S. Zarandi, and M. Rasti, "Joint resource allocation and offloading decision in mobile edge computing," *IEEE Commun. Lett.*, vol. 23, no. 4, pp. 684–687, Apr. 2019.

[26] J. Jalali and A. Khalili, "Optimal resource allocation for MC-NOMA in SWIPT-enabled networks," *IEEE Commun. Lett.*, vol. 24, no. 10, pp. 2250–2254, Oct. 2020.

[27] H. Tuy, "Monotonic optimization: Problems and solution approaches," *SIAM J. Optim.*, vol. 11, no. 2, pp. 464–494, Nov. 2000.

[28] H. Tuy, F. Al-Khayyal, and P. Thach, "Monotonic optimization: Branch and cut methods," in *Essays and Surveys in Global Optimization*, C. Audet, P. Hansen, and G. Savard, Eds. New York, NY, USA: Springer, 2005.

[29] E. Bjornson and E. Jorswieck, *Optimal Resource Allocation in Coordinated Multi-Cell Systems*. Boston, MA, USA: Now, Nov. 2012.

[30] A. Zappone, E. Björnson, L. Sanguinetti, and E. Jorswieck, "Globally optimal energy-efficient power control and receiver design in wireless networks," *IEEE Trans. Signal Process.*, vol. 65, no. 11, pp. 2844–2859, Jun. 2017.

[31] Y. J. Zhang, L. P. Qian, and J. Huang, "Monotonic optimization in communication and networking systems," *Found. Trends Netw.*, vol. 7, no. 1, pp. 1–75, Oct. 2013.

[32] Y. Sun, D. W. K. Ng, Z. Ding, and R. Schober, "Optimal joint power and subcarrier allocation for full-duplex multicarrier non-orthogonal multiple access systems," *IEEE Trans. Commun.*, vol. 65, no. 3, pp. 1077–1091, Mar. 2017.

[33] Y. Sun, D. W. K. Ng, J. Zhu, and R. Schober, "Robust and secure resource allocation for full-duplex MISO multicarrier NOMA systems," *IEEE Trans. Commun.*, vol. 66, no. 9, pp. 4119–4137, Sep. 2018.

[34] A. Khalili and D. W. K. Ng, "Energy and spectral efficiency tradeoff in OFDMA networks via antenna selection strategy," in *Proc. IEEE Wireless Commun. Netw. Conf. (WCNC)*, May 2020, pp. 1–6.

[35] A. Khalili, M. R. Mili, and D. W. K. Ng, "Performance trade-off between uplink and downlink in full-duplex communications," in *Proc. IEEE Int. Conf. Commun. (ICC)*, Jun. 2020, pp. 1–6.

[36] W. Dinkelbach, "On nonlinear fractional programming," *Manage. Sci.*, vol. 13, no. 7, pp. 492–498, Mar. 1967.

[37] S. Bayat, A. Khalili, and Z. Han, "Resource allocation for MC MISO-NOMA SWIPT-enabled HetNets with non-linear energy harvesting," *IEEE Access*, vol. 8, pp. 192270–192281, 2020.

[38] M. Grant, and S. Boyd. (Mar. 2014). *CVX: MATLAB Software for Disciplined Convex Programming, Version 2.1*. [Online]. Available: http://cvxr.com/cvx

[39] R. M. Radaydeh, F. S. Al-Qahtani, A. Celik, K. A. Qaraqe, and M.-S. Alouini, "Generalized imperfect D2D associations in spectrum-shared cellular networks under transmit power and interference constraints," *IEEE Access*, vol. 8, pp. 182517–182536, 2020.

[40] *3rd Generation Partnership Project; Technical Specification Group Radio Access Network; Evolved Universal Terrestrial Radio Access (EUTRA); Further Advancements for E-UTRA Physical Layer Aspects (Release 9)*, document 3GPP TR 36.814 V9.0.0, Mar. 2010.

SIAVASH BAYAT (Member, IEEE) received the B.Sc. and M.Sc. degrees in electrical engineering from Sharif University of Technology, Tehran, Iran, in 2002 and 2005, respectively, and the Ph.D. degree in electrical engineering from The University of Sydney, Australia, in 2013. He was then a Postdoctoral Research Fellow with The University of Sydney, prior to joining Sharif University of Technology, in 2014, where he is currently an Assistant Professor. From 2007 to 2009, he also was affiliated with Sharif University of Technology, where he held a Faculty Member position with responsibility for the research in wireless communication networks system design. His research interests include wireless resource management, wireless communications, the Internet of Things (IoT), signal processing, heterogeneous networks, sensor networks, cognitive radio, game theory, and physical layer security.

JALAL JALALI (Graduate Student Member, IEEE) received the M.Sc. degree in electrical engineering from Ghent University, Belgium, in 2020. He is currently pursuing the Ph.D. degree with the University of Antwerp, Belgium. His research interests include computational modeling, optimization methods, resource allocation in wireless communication, the Internet of Things (IoT) communication's standards, and localization systems.

ATA KHALILI (Member, IEEE) received the B.Sc. and M.Sc. degrees (Hons.) in electronic engineering and telecommunication engineering from Shahed University, in 2016 and 2018, respectively. From 2018 to 2019, he was a Visiting Researcher with the Department of Computer Engineering and Information Technology, Amirkabir University of Technology, Tehran, Iran. Since October 2019, he has been with the Department of Electrical and Computer Engineering, Tarbiat Modares University, Tehran, where he is currently a Research Assistant. He is also working as a Research Assistant with the Electronics Research Institute, Sharif University of Technology, Tehran. His research interests include intelligent reflecting surface (IRS), unmanned aerial vehicle (UAV) communications, resource allocation in wireless communication, green communication, mobile edge computing, and optimization theory. He served as a member of Technical Program Committees for the IEEE Globecom and IEEE WCNC Conference, in 2020, IEEE ICC, and IEEE Globecom, in 2021. He served as a Reviewer for several IEEE journals, such as IEEE Journal on Selected Areas in Communications and IEEE Transactions on Wireless Communications.

MOHAMMAD ROBAT MILI (Member, IEEE) received the Ph.D. degree in electrical and electronic engineering from The University of Manchester, U.K., in 2012. He held a postdoctoral research positions at the Department of Telecommunications and Information Processing, Ghent University, Belgium, and the Department of Electrical Engineering, Sharif University of Technology, Iran. His main research interests include design and analysis of wireless communication networks with particular focus on 5G cellular networks using mathematical methods, such as optimization theory, game theory, and machine learning.

SABINE WITTEVRONGEL received the master's degree in electrical engineering and the Ph.D. degree in engineering from Ghent University, Belgium, in 1992 and 1998, respectively. In 1992, she joined SMACS Research Group, Department of Telecommunications and Information Processing, Ghent University. Since 2001, she has been a Professor in the field of stochastic modeling and queuing analysis with the Faculty of Engineering and Architecture, Ghent University. Her main research interests include queuing theory, stochastic modeling and performance evaluation of communication networks, scheduling mechanisms, and energy-efficient protocols. In 1998, she received the Scientific Award Alcatel Bell for the work entitled ''Generic analytical techniques for the performance analysis of buffers in ATM networks.''

HEIDI STEENDAM (Senior Member, IEEE) received the M.Sc. degree in electrical engineering and the Ph.D. degree in applied sciences from Ghent University, Ghent, Belgium, in 1995 and 2000, respectively. Since 1995, she has been with the Digital Communications Research Group, Department of Telecommunications and Information Processing, Faculty of Engineering, Ghent University, in the framework of various research projects, and has been a Professor in digital communications, since 2002. In 2015, she was a Visiting Professor with Monash University. She has authored more than 150 scientific papers in international journals and conference proceedings, for which she received several best paper awards. Her main research interests include statistical communication theory, carrier and symbol synchronization, bandwidth-efficient modulation and coding, cognitive radio and cooperative networks, and positioning and visible light communication. She has been an Executive Committee Member of the IEEE Communications and Vehicular Technology Society Joint Chapter, Benelux Section, since 2002; the Vice Chair, since 2012; and the Chair, since 2017. She was active in various international conferences as a technical program committee chair/member and the session chair. In 2004 and 2011, she was the Conference Chair of the IEEE Symposium on Communications and Vehicular Technology in the Benelux. From 2012 to 2017, she was an Associate Editor of the IEEE Transactions on Communications and the *EURASIP Journal on Wireless Communications and Networking*.

• • •